

Large thermoelectric power and figure of merit in a ferromagnetic-quantum dot-superconducting device

Sun-Yong Hwang, Rosa López, and David Sánchez

Institut de Física Interdisciplinària i Sistemes Complexos IFISC (CSIC-UIB), E-07122 Palma de Mallorca, Spain

We investigate the thermoelectric properties of a quantum dot coupled to ferromagnetic and superconducting electrodes. The combination of spin polarized tunneling at the ferromagnetic-quantum dot interface and the application of an external magnetic field that Zeeman splits the dot energy level leads to large values of the thermopower (Seebeck coefficient). Importantly, the thermopower can be tuned with an external gate voltage connected to the dot. We compute the figure of merit that measures the efficiency of thermoelectric conversion and find that it attains high values. We discuss the different contributions from Andreev reflection processes and quasiparticle tunneling into and out of the superconducting contact. Furthermore, we obtain dramatic variations of both the magnetothermopower and the spin Seebeck effect, which suggest that in our device spin currents can be controlled with temperature gradients only.

I. INTRODUCTION

The quest for energy harvesting devices that efficiently convert waste heat into electricity has been intense in the last decades. It has been argued that low dimensional systems offer better performances due to interfacial boundary scattering of phonons [1] and strongly energy dependent transmissions [2]. The generated thermopower is given by the Seebeck coefficient S as the ratio between the created electric voltage and the temperature difference applied across the device with vanishing net current [3]. It turns out that electron-hole asymmetry present in the system determines the size of the thermoelectric effects given by S . The reason is that the electron and hole thermocurrents generated in response to a thermal gradient flow in opposite directions and for a particle-hole symmetric density of states (DOS) they exactly cancel each other, thus giving zero thermovoltage.

On the other hand, even if the Seebeck coefficient is large a heat current inevitably accompanies a temperature gradient. The efficiency of the thermoelectric process is then determined by the dimensionless figure of merit ZT , which accounts for the relation between the thermoelectric power factor and the heat or thermal conductance [4]. One would naively think that maximization of the figure of merit is expected in superconducting materials, which are perfect electric conductors and poor thermal conductors. However, the problem is that the superconducting DOS exhibits electron-hole symmetry and hence the thermopower is strongly suppressed [5].

Recent proposals suggest that electron-hole symmetry can be broken if the superconductor is put in proximity of ferromagnetic contacts [6] or by combining an external magnetic field with a spin filter [7]. The symmetry breaking originates from an exchange field induced splitting of the spin up and down energy subbands in the superconductor. As a consequence, large thermoelectric effects are predicted. The effect disappears if the spin polarization of the ferromagnetic side of the junction vanishes. A very recent work reports the observation of enhanced thermocurrents in superconductor-ferromagnet tunnel-coupled junctions [8]. Similarly, large values of the Seebeck coefficient are found in superconducting-normal bilayers with spin active inter-

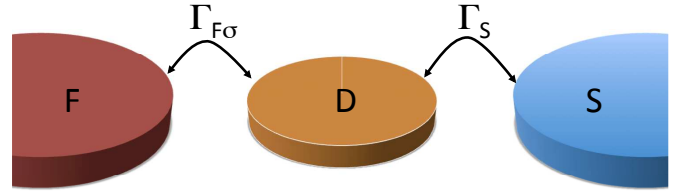


FIG. 1. (Color online) Schematic illustration of our device. A quantum dot (D) is sandwiched between the left electrode, which is hot and ferromagnetic (F), and the right reservoir, which is cold and superconducting (S). The tunnel couplings are indicated. We note that the hybridization between the source contact and the dot is spin dependent with $\sigma = \{\uparrow, \downarrow\}$. The energy level of the quantum dot can be tuned with a capacitively coupled gate terminal (not shown here).

faces [9] or if layered structures are considered [10].

Here, we propose to insert a quantum dot between the ferromagnetic source electrode and the superconducting drain contact as in Fig. 1. The advantage of the setup lies on the easy manipulation of the electron-hole symmetry in the local DOS by electrically coupling the dot to a nearby gate. The thermopower thus acquires a characteristic sawtooth structure as the gate potential sweeps across resonances in a semiconductor dot attached to normal leads [11, 12]. The gate voltage also controls the electron number in the dot. Furthermore, the sharp resonances in the dot allow us to play with energy filtering effects that may lead to an optimal thermoelectric conversion [13]. We find that the thermopower can be tuned between 0 and $350 \mu\text{V/K}$ when the energy level of the quantum dot is varied around the Fermi energy in the scale of the superconducting gap. Consequently, the figure of merit ZT increases from 0 up to 6.

The hybrid system considered here is also interesting for fundamental reasons. It is well known that at low bias voltages the dominant transport mechanism at the interface between a metal and a superconductor is an electron-hole conversion known as Andreev reflection [14]. The Andreev reflection generates a Cooper pair in the superconducting condensate and as such involves a spin flip process. Therefore, when the metal is ferromagnetic one expects a strong impact in the current-voltage characteristic of a ferromagnetic-

superconducting junction as a function of the magnetization distribution [15, 16]. One of the most spectacular effects is the appearance of drag currents in three-terminal structures as a result of cross Andreev processes [17–20]. Insertion of a large quantum dot increases the strength of the effect [21]. Additionally, ferromagnetic-quantum dot-superconducting systems serve as excellent platforms to study spin correlation effects [22].

Yet, we [23] recently pointed out that the Andreev current of a normal-quantum dot-superconducting device is zero to all orders in the temperature shift and therefore Andreev processes cannot alone generate finite thermovoltages due to the Onsager reciprocity relation [24, 25]. This also holds for a ferromagnetic contact, as we show below. Hence, it is crucial to take into account the role of quasiparticle currents. These appear when single electrons fill states in the source contact and can tunnel to empty quasiparticle states in the drain. The quasiparticle current [see Eq. (9) below] depends on the quasiparticle transmission [see Eq. (25) below], which is a function of superconducting density of states and changes abruptly on the scale of Δ . Therefore, we need Zeeman field splittings of the order of Δ to create abrupt changes in the thermopower. In addition, we observe enhanced values of the Seebeck coefficient for ferromagnet polarizations close to the half-metallic case because the Andreev conductance term sharply decreases when the polarization approaches 100 % and the thermopower thus increases [6]. The sensitivity of S to the polarization is also reflected in the magnetothermopower, which shows strong variations as a function of the energy level and the Zeeman splitting upon reversal of the magnetization. Remarkably, we find very large values of ZT as a result of the combined effect of external magnetic fields, spin polarization and appropriate tuning of the dot energy level.

We also explore spin caloritronic effects that arise when a spin polarized current is generated under the influence of a temperature bias [26–28]. For Andreev processes we below demonstrate that the spin current vanishes even if Zeeman splittings or spin-dependent tunnel couplings are present. This is valid even in nonequilibrium conditions (finite voltage and temperature biases) and is due to a symmetry between the electron and hole sectors. However, the quasiparticle current is free from this constraint and we expect, quite generally, nonzero spin currents in temperature driven junctions. A way to quantify thermally generated spin voltages is to define the spin Seebeck coefficient S_s . It is natural that when the ferromagnet polarization and the external magnetic field are zero the spin thermopower vanishes. Nevertheless, we obtain values of S_s as large as $500 \mu\text{V/K}$ in the presence of Zeeman splittings and nonzero magnetization. Our findings thus suggest that a ferromagnetic-quantum dot-superconducting device is a good candidate to create large spin population imbalances using thermal means only.

The paper is organized as follows. In Sec. II, we explain the theoretical model. The magnetization in the ferromagnetic contact leads to spin-dependent tunneling rates for the ferromagnetic-quantum dot coupling. We discuss both the electric current and the heat flux driven by voltage or temperature biases and separate the contributions from Andreev

processes and quasiparticle tunneling. In Sec. III we give the transport coefficients (electric, thermoelectric, electrothermal and thermal conductances) that characterize the linear transport regime. We show that the cross responses obey the Kelvin-Onsager relation. We also derive appropriate expressions for the charge thermopower, the figure of merit and the spin Seebeck coefficient. Section IV contains our main results. We discuss the dependence of the thermoelectric effects for both charge and spin on the spin polarization, the applied magnetic field and the external gate voltage. Finally, we summarize our findings in Sec. V.

II. HAMILTONIAN AND GREEN'S FUNCTION APPROACH

The F-D-S device is comprised of the left ferromagnet (F) with a polarization p ($|p| \leq 1$), a single-level quantum dot (D), and the right superconductor (S) as depicted in Fig. 1. The total Hamiltonian reads

$$\mathcal{H} = \mathcal{H}_F + \mathcal{H}_S + \mathcal{H}_D + \mathcal{H}_T, \quad (1)$$

where

$$\mathcal{H}_F = \sum_{k\sigma} \varepsilon_{Fk\sigma} c_{Fk\sigma}^\dagger c_{Fk\sigma} \quad (2)$$

describes the charge carrier with momentum k , spin σ with a magnetization $M\sigma$ along the given axis (say z) in the left ferromagnet and

$$\mathcal{H}_S = \sum_{k\sigma} \varepsilon_{Sk\sigma} c_{Sk\sigma}^\dagger c_{Sk\sigma} + \sum_k [\Delta c_{S,-k\uparrow}^\dagger c_{Sk\downarrow}^\dagger + \text{H.c.}] \quad (3)$$

describes the right superconductor with an order parameter given by the energy gap Δ . We neglect the phase of Δ and treat it as a real constant. This is valid with a suitable gauge transformation when we consider an equilibrium superconductor. In what follows, we set $\Delta = 1$ as an energy unit. In the dot Hamiltonian

$$\mathcal{H}_D = \sum_{\sigma} \varepsilon_{d\sigma} d_{\sigma}^\dagger d_{\sigma}, \quad (4)$$

the spin-degenerate energy level can be split when the magnetic field is on, i.e., $\varepsilon_{d\sigma} = \varepsilon_d + \sigma\Delta_Z$ with Zeeman splitting Δ_Z . Scattering at the ferromagnet creates spin-dependent scattering phases that to first order induce an additional effective Zeeman splitting and can be included into Δ_Z [29]. Finally, the charge tunneling between the quantum dot and each lead is described by

$$\mathcal{H}_T = \sum_{k\sigma} t_{F\sigma} c_{Fk\sigma}^\dagger d_{\sigma} + \sum_{k\sigma} t_{S\sigma} c_{Sk\sigma}^\dagger d_{\sigma} + \text{H.c.} \quad (5)$$

We ignore spin-flip scattering (see, however, Ref. [30]) and evaluate the spin-resolved charge and heat currents from the time evolution of spin- σ electron number $N_{F\sigma} =$

$\sum_k c_{Fk\sigma}^\dagger c_{Fk\sigma}$ and the energy $\mathcal{H}_{F\sigma} = \sum_k \varepsilon_{Fk\sigma} c_{Fk\sigma}^\dagger c_{Fk\sigma}$ in the left ferromagnet

$$I_\sigma = -(ie/\hbar)\langle[\mathcal{H}, N_{F\sigma}]\rangle, \quad (6)$$

$$J_\sigma = -(i/\hbar)\langle[\mathcal{H}, \mathcal{H}_{F\sigma}]\rangle - I_\sigma V, \quad (7)$$

where the last term corresponds to the Joule heating. Applying the nonequilibrium Keldysh-Green formalism [31, 32], we find that the current for each spin $I_\sigma = I_A^\sigma + I_Q^\sigma$ is given by a sum of two terms, i.e., the spin-resolved Andreev current I_A^σ and that of quasiparticle contribution I_Q^σ in terms of their corresponding transmission probabilities T_A^σ and T_Q^σ ,

$$I_A^\sigma = \frac{e}{\hbar} \int d\varepsilon T_A^\sigma(\varepsilon) [f_F(\varepsilon - eV) - f_F(\varepsilon + eV)], \quad (8)$$

$$I_Q^\sigma = \frac{e}{\hbar} \int d\varepsilon T_Q^\sigma(\varepsilon) [f_F(\varepsilon - eV) - f_S(\varepsilon)], \quad (9)$$

where $f_{\alpha=F,S}(\varepsilon \pm eV) = \{1 + \exp[(\varepsilon \pm eV - E_F)/k_B T_\alpha]\}^{-1}$ is the Fermi-Dirac distribution with the applied voltage $V = V_F - V_S$ and the electrode temperature $T_\alpha = T + \theta_\alpha$ (T : background temperature, θ_α : thermal bias). For definiteness, we drive only the F lead assuming that the right superconductor is at equilibrium ($V_S = \theta_S = 0$) and take the Fermi level as the energy reference ($E_F = 0$). Similarly, the heat current is given by $J_\sigma = J_A^\sigma + J_Q^\sigma$ with

$$J_A^\sigma = -2V I_A^\sigma, \quad (10)$$

$$J_Q^\sigma = \frac{1}{\hbar} \int d\varepsilon (\varepsilon - eV) T_Q^\sigma(\varepsilon) [f_F(\varepsilon - eV) - f_S(\varepsilon)]. \quad (11)$$

In Eq. (10), the Andreev energy flow cancels out due to the particle-hole (p - h) symmetry and only the Joule part survives. In other words, we have

$$J_{A\sigma}^{(p)} = \frac{1}{\hbar} \int d\varepsilon (\varepsilon - eV) T_A^\sigma(\varepsilon) [f_F(\varepsilon - eV) - f_F(\varepsilon + eV)], \quad (12)$$

and

$$J_{A\sigma}^{(h)} = \frac{1}{\hbar} \int d\varepsilon (\varepsilon + eV) T_A^\sigma(\varepsilon) [f_F(\varepsilon + eV) - f_F(\varepsilon - eV)]. \quad (13)$$

Hence $J_A^\sigma = J_{A\sigma}^{(p)} + J_{A\sigma}^{(h)} = -2V I_A^\sigma$. Importantly, this property causes the Andreev heat current to vanish in the linear response regime when we apply a small voltage bias (i.e., no Peltier effect). Note that the factor 2 in Eq. (10) comes from an equal contribution of particle and hole to the heat current.

The key quantities to determine the transmission probabilities T_A^σ and T_Q^σ are the dot retarded Green's functions $G_{ij}^r(\varepsilon)$ ($i, j = 1, 2, 3, 4$) calculated in the spin-generalized Nambu spinor basis $\hat{d} = (d_\uparrow, d_\downarrow, d_\downarrow^\dagger, d_\uparrow^\dagger)^T$

$$\mathbf{G}_d^r(\varepsilon) = \begin{pmatrix} G_{11}^r(\varepsilon) & G_{12}^r(\varepsilon) & 0 & 0 \\ G_{21}^r(\varepsilon) & G_{22}^r(\varepsilon) & 0 & 0 \\ 0 & 0 & G_{33}^r(\varepsilon) & G_{34}^r(\varepsilon) \\ 0 & 0 & G_{43}^r(\varepsilon) & G_{44}^r(\varepsilon) \end{pmatrix}, \quad (14)$$

where 2×2 submatrices in the first block ($i, j = 1, 2$) and the second block ($i, j = 3, 4$) correspond to the electron spin-up and spin-down spaces respectively, with subscripts 1, 3 denoting electron sectors and 2, 4 referring to hole parts. The whole matrix in Eq. (14) is block-diagonal since we have ignored spin-flip processes, which thus separates the spin spaces. The Green's functions are explicitly given by [30, 32]

$$G_{11}^r = \left[\varepsilon - \varepsilon_{d\uparrow} + \frac{i\Gamma_{F\uparrow}}{2} + \frac{i\Gamma_S}{2} \beta_d(\varepsilon) + \frac{\Gamma_S^2 \Delta^2 A_1^r(\varepsilon)}{4(\varepsilon^2 - \Delta^2)} \right]^{-1}, \quad (15)$$

$$G_{33}^r = \left[\varepsilon - \varepsilon_{d\downarrow} + \frac{i\Gamma_{F\downarrow}}{2} + \frac{i\Gamma_S}{2} \beta_d(\varepsilon) + \frac{\Gamma_S^2 \Delta^2 A_2^r(\varepsilon)}{4(\varepsilon^2 - \Delta^2)} \right]^{-1}, \quad (16)$$

$$G_{12}^r = G_{21}^r = G_{11}^r \frac{i\Gamma_S}{2} \beta_o(\varepsilon) A_1^r(\varepsilon), \quad (17)$$

$$G_{34}^r = G_{43}^r = -G_{33}^r \frac{i\Gamma_S}{2} \beta_o(\varepsilon) A_2^r(\varepsilon), \quad (18)$$

with

$$A_1^r(\varepsilon) = \left[\varepsilon + \varepsilon_{d\downarrow} + \frac{i\Gamma_{F\downarrow}}{2} + \frac{i\Gamma_S}{2} \beta_d(\varepsilon) \right]^{-1}, \quad (19)$$

$$A_2^r(\varepsilon) = \left[\varepsilon + \varepsilon_{d\uparrow} + \frac{i\Gamma_{F\uparrow}}{2} + \frac{i\Gamma_S}{2} \beta_d(\varepsilon) \right]^{-1}, \quad (20)$$

$$\beta_d(\varepsilon) = \frac{\Theta(|\varepsilon| - \Delta)|\varepsilon|}{\sqrt{\varepsilon^2 - \Delta^2}} - i \frac{\Theta(\Delta - |\varepsilon|)\varepsilon}{\sqrt{\Delta^2 - \varepsilon^2}}, \quad (21)$$

$$\beta_o(\varepsilon) = \frac{\Theta(|\varepsilon| - \Delta)\text{sgn}(\varepsilon)\Delta}{\sqrt{\varepsilon^2 - \Delta^2}} - i \frac{\Theta(\Delta - |\varepsilon|)\Delta}{\sqrt{\Delta^2 - \varepsilon^2}}. \quad (22)$$

The remaining Green's functions follow from Eqs. (15) and (16): $G_{22}^r(\varepsilon) = -G_{33}^{r,*}(-\varepsilon)$ and $G_{44}^r(\varepsilon) = -G_{11}^{r,*}(-\varepsilon)$. We have used the wide band approximation, i.e., energy-independent tunnel couplings, $\Gamma_{F\sigma} = \Gamma_F(1 + \sigma p) = 2\pi|t_{F\sigma}|^2 \sum_k \delta(\varepsilon - \varepsilon_{Fk\sigma})$ and $\Gamma_{S\sigma} = \Gamma_S = 2\pi|t_{S\sigma}|^2 \sum_p \delta(\varepsilon - \varepsilon_{Sp\sigma})$ with $\Gamma_\alpha = (\Gamma_{\alpha\uparrow} + \Gamma_{\alpha\downarrow})/2$ being the spin-averaged coupling constant to each lead $\alpha = F, S$. The spin dependence in $\Gamma_{F\sigma}$ arises from the nonzero magnetization in the ferromagnet,

$$p = \frac{\nu_\uparrow - \nu_\downarrow}{\nu_\uparrow + \nu_\downarrow}, \quad (23)$$

where $\nu_\sigma = \sum_k \delta(\varepsilon - \varepsilon_{Fk\sigma})$ is the ferromagnet density of states. We wish to point out that for $p = \Delta_Z = 0$ the spin dependence of the system disappears as we would end up with a normal-quantum dot-superconducting setup [33, 34]. Possible spintronic (or spin caloritronic) nature can only emerge with a nonzero polarization or a magnetic field, or the combination of both, either $p \neq 0$ or $\Delta_Z \neq 0$.

One can write the spin-resolved Andreev transmission in terms of Green's functions, viz.

$$T_A^\uparrow(\varepsilon) = \Gamma_{F\uparrow} \Gamma_{F\downarrow} |G_{12}^r(\varepsilon)|^2, \quad (24a)$$

$$T_A^\downarrow(\varepsilon) = \Gamma_{F\downarrow} \Gamma_{F\uparrow} |G_{34}^r(\varepsilon)|^2, \quad (24b)$$

with which the Andreev charge $I_A^c = I_A^\uparrow + I_A^\downarrow$ and spin $I_A^s = I_A^\uparrow - I_A^\downarrow$ currents can be defined via Eq. (8). The Andreev

heat flux $J_A^c = -2VI_A^c$ and the spin-polarized one $J_A^s = -2VI_A^s$ can be determined from Eq. (10). Analogously, the quasiparticle charge and spin currents (and those of heat) are respectively given by $I_Q^c = I_Q^\uparrow + I_Q^\downarrow$ ($J_Q^c = J_Q^\uparrow + J_Q^\downarrow$) and $I_Q^s = I_Q^\uparrow - I_Q^\downarrow$ ($J_Q^s = J_Q^\uparrow - J_Q^\downarrow$) with the aid of Eqs. (9) and (11) and the corresponding transmissions

$$T_Q^\uparrow(\varepsilon) = \Gamma_{F\uparrow}\tilde{\Gamma}_S \left(|G_{11}^r|^2 + |G_{12}^r|^2 - \frac{2\Delta}{|\varepsilon|} \text{Re}[G_{11}^r G_{12}^{r,*}] \right), \quad (25a)$$

$$T_Q^\downarrow(\varepsilon) = \Gamma_{F\downarrow}\tilde{\Gamma}_S \left(|G_{33}^r|^2 + |G_{34}^r|^2 + \frac{2\Delta}{|\varepsilon|} \text{Re}[G_{33}^r G_{34}^{r,*}] \right), \quad (25b)$$

where $\tilde{\Gamma}_S = \Gamma_S \Theta(|\varepsilon| - \Delta) |\varepsilon| / \sqrt{\varepsilon^2 - \Delta^2}$.

For $p = \Delta_Z = 0$, one can easily show that $G_{11}^r(\varepsilon) = G_{33}^r(\varepsilon)$ and $G_{12}^r(\varepsilon) = -G_{34}^r(\varepsilon)$, hence $T_A^\uparrow(\varepsilon) = T_A^\downarrow(\varepsilon)$ and $T_Q^\uparrow(\varepsilon) = T_Q^\downarrow(\varepsilon)$ from Eqs. (24) and (25) respectively. In this case all the spin currents vanish identically, $I_A^s = I_Q^s = J_A^s = J_Q^s = 0$, as expected. If either $p \neq 0$ or $\Delta_Z \neq 0$, the spin symmetry is generally broken, i.e., $T_A^\uparrow(\varepsilon) \neq T_A^\downarrow(\varepsilon)$ and $T_Q^\uparrow(\varepsilon) \neq T_Q^\downarrow(\varepsilon)$, leading to a spin-polarized net current. Nevertheless, focusing on Andreev transport only, the inherent particle-hole symmetry strictly satisfies $T_A^\uparrow(\varepsilon) = T_A^\downarrow(-\varepsilon)$ even in nonequilibrium conditions. Then, it follows from Eqs. (8) and (10) that $I_A^s = J_A^s = 0$ due to the symmetry of integrands in energy space, i.e.,

$$I_A^s = \frac{e}{h} \int d\varepsilon [T_A^\uparrow(\varepsilon) - T_A^\downarrow(\varepsilon)] [f_F(\varepsilon - eV) - f_F(\varepsilon + eV)] = 0, \quad (26)$$

with the property $f_F(-\varepsilon \pm eV) = 1 - f_F(\varepsilon \mp eV)$ (recall that we take $E_F = 0$). Therefore, in our model the subgap Andreev process always prohibits the generation of spin-polarized currents. Spin dependence of the crossed Andreev transport can be observed in the strong coupling regime with a multiterminal device [35] but here we consider a two-terminal device.

In stark contrast, I_Q^s and J_Q^s are generally nonzero with a finite p or Δ_Z [see Eqs. (9), (11), and (25)]. Thus, net spin currents arise only from the quasiparticle contributions $I_s = I_Q^s$ and $J_s = J_Q^s$. On the other hand, the total charge current $I_c = I_\uparrow + I_\downarrow$ and the total heat flux $J_c = J_\uparrow + J_\downarrow$ in general consist of the sum of both the Andreev parts and the quasiparticle contributions. Hence, we can write without loss of generality

$$I_c = I_A^c + I_Q^c, \quad (27)$$

$$I_s = I_Q^s, \quad (28)$$

and for the heat

$$J_c = J_A^c + J_Q^c, \quad (29)$$

$$J_s = J_Q^s. \quad (30)$$

III. LINEAR THERMOELECTRIC TRANSPORT

As can be seen in Eq. (8), the spin-resolved Andreev current I_A^σ has no response to a thermal driving in the isoelectric case $V = 0$ [23], and in the linear regime we only have the contribution $I_A^\sigma = G_A^\sigma V$ with zero thermoelectric conductance. Accordingly, the Andreev heat flux J_A^σ in Eq. (10) has no linear term (the first nonzero term is quadratic). Thus, in linear response the spin-resolved charge and heat currents become

$$I_\sigma = (G_A^\sigma + G_Q^\sigma)V + L_Q^\sigma \theta, \quad (31)$$

$$J_\sigma = R_Q^\sigma V + K_Q^\sigma \theta, \quad (32)$$

with the corresponding transport coefficients given by

$$G_A^\sigma = \frac{2e^2}{h} \int d\varepsilon (-\partial_\varepsilon f) T_A^\sigma, \quad (33)$$

$$G_Q^\sigma = \frac{e^2}{h} \int d\varepsilon (-\partial_\varepsilon f) T_Q^\sigma, \quad (34)$$

$$L_Q^\sigma = \frac{e}{h} \int d\varepsilon \frac{\varepsilon - E_F}{T} (-\partial_\varepsilon f) T_Q^\sigma, \quad (35)$$

$$R_Q^\sigma = \frac{e}{h} \int d\varepsilon (\varepsilon - E_F) (-\partial_\varepsilon f) T_Q^\sigma, \quad (36)$$

$$K_Q^\sigma = \frac{1}{h} \int d\varepsilon \frac{(\varepsilon - E_F)^2}{T} (-\partial_\varepsilon f) T_Q^\sigma, \quad (37)$$

where $\partial_\varepsilon f$ denotes the energy derivative of Fermi function at equilibrium ($V_\alpha = \theta_\alpha = 0$). Equation (29) further reduces to $J_c = J_Q^c$ as there is no Andreev contribution in Eq. (32) which only appears in the nonlinear transport regime [Eq. (10)]. Moreover, this vanishing linear Andreev heat current with V is fundamentally linked to the Kelvin-Onsager relation, implying that the absence of L_A^σ in Eq. (31) due to the inherent particle-hole symmetry also guarantees the absence of R_A^σ in Eq. (32). For the quasiparticle coefficients, we find $R_Q^\sigma(p, \Delta_Z) = TL_Q^\sigma(-p, -\Delta_Z)$ since the transmission obeys the relation $T_{A,Q}^\sigma(p, \Delta_Z) = T_{A,Q}^\sigma(-p, -\Delta_Z)$ due to microreversibility. This also implies $X^\sigma(p, \Delta_Z) = X^\sigma(-p, -\Delta_Z)$ for all the kinetic coefficients $X = G, L, R, K$. Furthermore, we obtain $R_Q^\sigma = TL_Q^\sigma$ as one can easily verify from Eqs. (35) and (36).

Employing Eqs. (31) and (32), we write the linear response charge and heat currents as

$$I_c = \sum_\sigma \left[(G_A^\sigma + G_Q^\sigma)V + L_Q^\sigma \theta \right], \quad (38)$$

$$J_c = \sum_\sigma \left[R_Q^\sigma V + K_Q^\sigma \theta \right], \quad (39)$$

and the spin-polarized counterparts as

$$I_s = (G_Q^\uparrow - G_Q^\downarrow)V + (L_Q^\uparrow - L_Q^\downarrow)\theta, \quad (40)$$

$$J_s = (R_Q^\uparrow - R_Q^\downarrow)V + (K_Q^\uparrow - K_Q^\downarrow)\theta, \quad (41)$$

where we have used the symmetry relation $G_A^\uparrow = G_A^\downarrow$ in Eq. (40). Notice that Eqs. (40) and (41) are consistent with

Eqs. (28) and (30) when the linear response regime is considered.

The linear responses found above completely determine the thermoelectric properties of our device. Let us first focus on the charge transport. The Seebeck coefficient or thermopower is defined as the generated voltage from thermal gradients in open circuit conditions $I_c = 0$. This can be easily evaluated from Eq. (38):

$$S = -\frac{V}{\theta} \Big|_{I_c=0} = \frac{\sum_{\sigma} L_Q^{\sigma}}{\sum_{\sigma} (G_A^{\sigma} + G_Q^{\sigma})}. \quad (42)$$

The efficiency of the thermoelectric conversion can be quantified by the figure of merit ZT . We first calculate the thermal conductance with the help of Eqs. (38) and (39):

$$\kappa = \frac{J_c}{\theta} \Big|_{I_c=0} = \sum_{\sigma} K_Q^{\sigma} - \frac{1}{T} \frac{(\sum_{\sigma} R_Q^{\sigma})^2}{\sum_{\sigma} (G_A^{\sigma} + G_Q^{\sigma})}, \quad (43)$$

Then, we find

$$ZT = \frac{GS^2T}{\kappa} = \frac{\sum_{\sigma} (G_A^{\sigma} + G_Q^{\sigma}) S^2 T}{\sum_{\sigma} K_Q^{\sigma} - TS \sum_{\sigma} L_Q^{\sigma}}, \quad (44)$$

where we have used Eq. (42) and the Kelvin-Onsager relation in order to rewrite Eq. (43). This expression clearly shows that a way to enhance the value of ZT is to get higher S . In deriving Eq. (43) we have assumed that energy is carried by electronic degrees of freedom only. We thus disregard the role of phonons, which can be nonnegligible at intermediate values of the background temperature T .

We now turn to the spin-dependent transport. Quite generally, spin-dependent tunneling due to $\Gamma_{F\sigma}$ leads to spin accumulations in the F side. It will spin split the chemical potential of the magnetic reservoir. If the size of the electrode is not sufficiently large and the spin-relaxation time is long, we will have a nonzero spin bias V_s . Then, Eqs. (38) and (40) are generalized as (let $G_{\sigma} = G_A^{\sigma} + G_Q^{\sigma}$)

$$I_c = (G_{\uparrow} + G_{\downarrow})V + \frac{1}{2}(G_{\uparrow} - G_{\downarrow})V_s + (L_Q^{\uparrow} + L_Q^{\downarrow})\theta, \quad (45)$$

$$I_s = (G_{\uparrow} - G_{\downarrow})V + \frac{1}{2}(G_{\uparrow} + G_{\downarrow})V_s + (L_Q^{\uparrow} - L_Q^{\downarrow})\theta. \quad (46)$$

From these expressions one can determine the spin Seebeck coefficient

$$S_s = -\frac{V_s}{\theta} \Big|_{I_c=0, I_s=0} = \frac{L_Q^{\uparrow}}{G_A^{\uparrow} + G_Q^{\uparrow}} - \frac{L_Q^{\downarrow}}{G_A^{\downarrow} + G_Q^{\downarrow}}, \quad (47)$$

which measures the generated spin voltage from the application of a temperature difference θ when both the charge and the spin currents vanish. These conditions give a constraint for the applied voltage. Alternative definitions of S_s are also possible [36]. Here, we have chosen the condition $I_c = 0$ and $I_s = 0$ because it is a natural extension to the theoretical proposal of charge Seebeck case in an open circuit [37].

Another important aspect of spin transport is the dependence of the thermopower on the magnetization or the applied

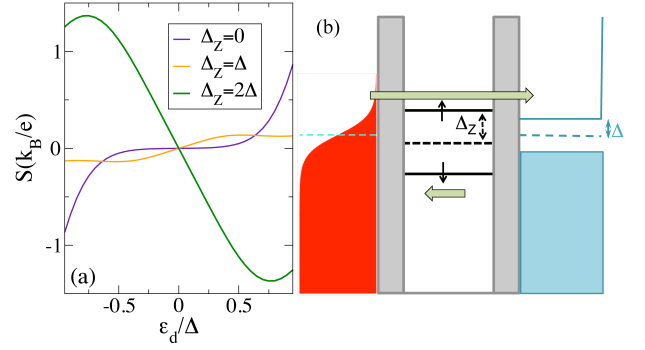


FIG. 2. (Color online) (a) Thermopower (charge Seebeck coefficient) S versus the level position ε_d at $p = 0$ and background temperature $k_B T = 0.2\Delta$ for several values of the Zeeman splitting Δ_Z . We use $\Gamma_F = 0.1\Delta$ and $\Gamma_S = 0.5\Delta$, i.e., the ferromagnet is the probe terminal, here and throughout the paper. (b) Energy diagram for a resonant tunneling double barrier system (the dot) coupled between the normal metal (left) and a superconducting reservoir (right) with $\varepsilon_d < 0$ (dashed black line), $E_F = 0$ (dashed blue line), $\Delta_Z = 2\Delta$ (solid black lines) and $p = 0$ (normal case). The hot metal displays a thermally smeared state distribution (red). At very low temperature, the cold superconductor (blue) has empty quasiparticle states above the gap Δ . The filled states below Δ are represented with solid blue. Note that the current due to temperature excited electrons from the left electrode (right arrow) is much larger than the opposite flow of electrons (left arrow), which is mostly blocked by filled states in the normal lead for $\varepsilon_d < E_F$. Asymmetric size of the left and right arrows indicates the spin-dependent particle-hole asymmetry generated by gating the dot and reinforced by Zeeman splitting. Accordingly, the net thermoelectric current due to a temperature difference is large.

magnetic field [38]. We can then define the magneto-Seebeck coefficients MS_p and MS_Z , which measure variations in the thermopower when p and Δ_Z are reversed, respectively:

$$MS_p = S(p) - S(-p), \quad (48)$$

$$MS_Z = S(\Delta_Z) - S(-\Delta_Z). \quad (49)$$

IV. RESULTS AND DISCUSSION

The above formulas are general and can be applied to a variety of situations. In this section, we consider the case where the dot is more strongly coupled to the superconducting lead ($\Gamma_F = 0.1\Delta$ and $\Gamma_S = 0.5\Delta$). This amplifies the effects discussed below but qualitatively the physics remains the same if the opposite situation (ferromagnetic dominant case) is considered.

Our results rely on the breaking of particle-hole symmetry. This can be done in three different ways. First, the gating of the quantum dot energy level ε_d away from the Fermi energy breaks the symmetry and thus creates a finite thermoelectric signal. Second, the Zeeman field splitting Δ_Z can enhance the effect of gate potential if one of the spin split levels is shifted out of the gap region. Third, the spin polarization p of ferromagnetic lead causes an asymmetry in the electron and hole transport in case of spin-split dot levels.

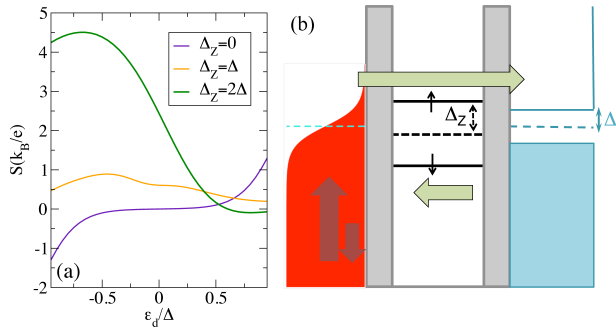


FIG. 3. (Color online) (a) S versus ε_d at $p = 0.9$ and $k_B T = 0.2\Delta$ for several Δ_Z . (b) Energy diagram analogous to Fig. 2(b) but with a ferromagnetic electrode (different spin populations are indicated with vertical arrows). Since more electrons with spin up are now available for tunneling, the thermocurrent increases as compared to the normal case in Fig. 2(b).

Figure 2(a) presents the charge thermopower as a function of the dot level position ε_d for various Zeeman splittings Δ_Z and magnetization $p = 0$. At the symmetric point when the dot level is aligned with the Fermi energy, the Seebeck coefficient S vanishes independently of Δ_Z . We observe that S is close to zero for most values of the dot level within the gap if both p and Δ_Z are zero. As discussed above, we thus need to break the particle-hole symmetry in the system by the simultaneous application of nonzero Δ_Z and ε_d . When Δ_Z is of the order of the superconducting gap, the thermopower increases as compared with the $\Delta_Z = 0$ case but the effect is more dramatic when $\Delta_Z = 2\Delta$. The thermopower attains large negative (positive) values for positive (negative) ε_d . This can be understood from the energy diagram shown in Fig. 2(b) where we depict the case of a large Zeeman splitting and a negative ε_d . Due to the energy dependence of the superconducting density of states, the level $\varepsilon_{d\downarrow}$ lies in a region with a small number of available states. Transport then takes place mainly across the upper $\varepsilon_{d\uparrow}$ level. Since this leads to a positive thermocurrent [large arrow in Fig. 2(b)], the definition of Eq. (42) implies that the thermopower is thus positive. Remarkably, our device shows great values of $|S|$ even if $p = 0$, which clearly differs from ferromagnet-superconductor junctions where the thermoelectric effect is predicted to vanish if $p = 0$ [7].

The case of nonzero magnetization is illustrated in Fig. 3(a). The thermopower is largely enhanced when the Zeeman splitting increases. In comparison with Fig. 2(a) we find that the combination of magnetic fields and ferromagnetic contacts leads to values of S of the order of 4 (in units of $k_B/e = 86 \mu\text{V/K}$) for certain values of the dot level. This increase is clarified in Fig. 3(b). Because there exist more electrons with spin \uparrow in the left lead, the thermocurrent increases since more electrons are able to tunnel through the upper dot level and the thermopower, which is proportional to the thermoelectric conductance, thus grows [cf. the case $p = 0$ in Fig. 2(b)]. On the other hand, the relatively small values of S for positive ε_d can be explained from a compensation effect. If $\varepsilon_d > 0$ the energetically favorable channel is $\varepsilon_{d\downarrow}$ but few electrons with

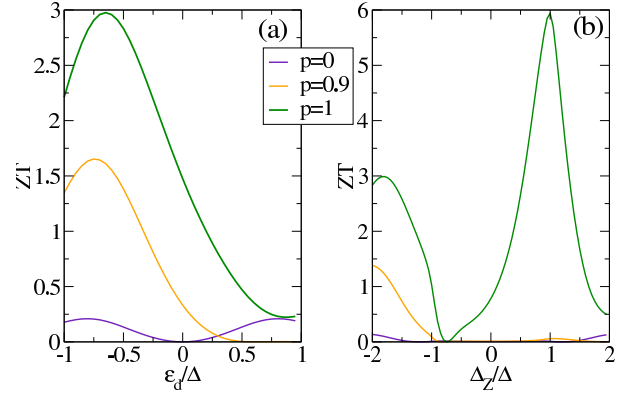


FIG. 4. (Color online) Thermoelectric figure of merit ZT versus (a) ε_d at $\Delta_Z = 2\Delta$ and (b) Δ_Z at $\varepsilon_d = 0.5\Delta$ for several polarization values of the ferromagnetic electrode at $k_B T = 0.2\Delta$.

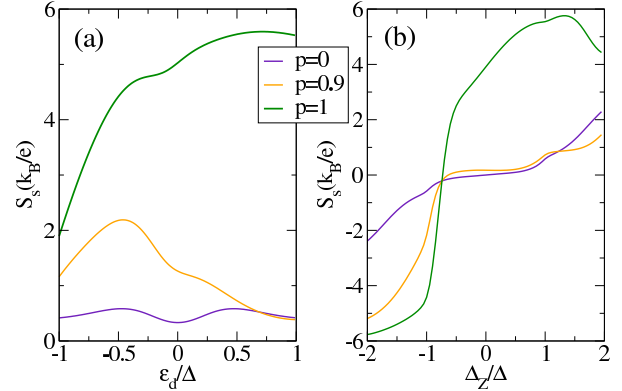


FIG. 5. (Color online) Spin Seebeck coefficient S_s versus (a) ε_d at $\Delta_Z = \Delta$ and (b) Δ_Z at $\varepsilon_d = 0.5\Delta$ for several polarization values of the ferromagnetic electrode at $k_B T = 0.2\Delta$.

spin \downarrow are available as $p = 0.9$. Therefore, I_c decreases and the generated thermovoltage is low. This demonstrates that thermoelectric effects can be highly tunable by changing the gate potential applied to the dot.

The thermoelectric figure of merit calculated from Eq. (44) is displayed in Fig. 4(a). Its behavior follows the thermopower properties discussed above. ZT increases for negative ε_d when both p and Δ_Z are positive and large. The exact value of ZT can be also tuned at a fixed position of the dot level. This is illustrated in Fig. 4(b), where the figure of merit reaches very high values as a function of the applied magnetic field, especially in the half-metallic case ($p = 1$). Our results thus show that a F-D-S device may act as an efficient waste heat-to-electric energy generator. Furthermore, this system could also be useful for cooling applications at very low temperature since Peltier and Seebeck effects are reversible.

The spin Seebeck coefficient S_s is calculated from Eq. (47).

V. CONCLUSIONS

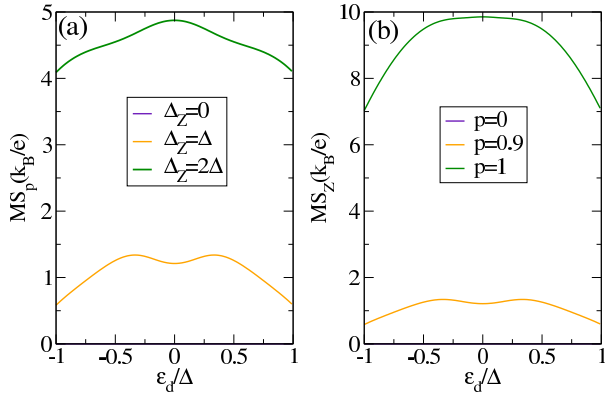


FIG. 6. (Color online) Magneto-Seebeck coefficients (a) MS_p at $p = 0.9$ and (b) MS_Z at $\Delta_Z = \Delta$ as a function of the dot level position for $k_B T = 0.2\Delta$.

In Fig. 5(a) we show the results as a function of the dot level for fixed Zeeman splitting and increasing values of the ferromagnet polarization. We find that S_s increases with p and reaches high values in the half-metallic case. The spin Seebeck coefficient is always positive because in the right-hand side of Eq. (47) the first term, which corresponds to electrons with spin \uparrow , dominates over the second term. In fact, L_Q^\uparrow grows as p increases since more electrons with spin \uparrow are available for tunneling whereas at the same time L_Q^\downarrow decreases. In the analysis of S_s as a function of the Zeeman splitting keeping ε_d constant [Fig. 5(b)], we obtain an interesting change of sign. For positive Δ_Z the spin Seebeck coefficient is positive for the reasons discussed above. However, for sufficiently negative values of Δ_Z , S_s becomes negative since now $\varepsilon_{d\uparrow}$ lies below the Fermi energy and L_Q^\uparrow then changes sign while L_Q^\downarrow is still close to zero for large values of p . In any case, the results for $|S_s|$ are large provided the Zeeman splitting is of the same order as the superconducting gap.

Both the magneto-Seebeck coefficients MS_p and MS_Z as defined in Eqs. (48) and (49) are respectively plotted in Figs. 6(a) and 6(b) as a function of the dot level position. For MS_p we fix $p = 0.9$ and vary the Zeeman splitting while for MS_Z we set $\Delta_Z = \Delta$ and change the ferromagnetic polarization. Strikingly, all curves show a characteristic symmetry with regard to the Fermi energy. In the case of MS_p this is understood from the relation $S(p, \varepsilon_d) = -S(-p, -\varepsilon_d)$ for a given Δ_Z . Physically, it means that an electron-hole transformation that shifts the dot level with respect to $E_F = 0$ and simultaneously reverses the ferromagnetic polarization induces a thermocurrent with the opposite sign. This can be seen in Fig. 2(a) for $p = 0$. In the case of MS_Z , a similar symmetry relation holds, namely, $S(\Delta_Z, \varepsilon_d) = -S(-\Delta_Z, -\varepsilon_d)$. Overall, both magneto-Seebeck coefficients increase for larger Zeeman splittings or ferromagnetic polarizations, in agreement with our previous results.

We have investigated the thermoelectric properties of a ferromagnetic-quantum dot-superconducting device in the presence of an external magnetic field applied to the dot. We have shown that the device develops high values of the thermopower from the combined effect of spin polarized tunneling, Zeeman splitting and tuning of the dot level. Importantly, the thermoelectric conversion is efficient since the dimensionless figure of merit reaches values as high as 6. Moreover, the spin Seebeck effect exhibits relevant changes as a function of the gate potential and the magneto-Seebeck coefficient becomes sensitive with reversals of the magnetization direction or the applied magnetic field.

Our predictions can be tested with today's experimental techniques. The quantum dot can be formed inside a carbon nanotube attached to ferromagnetic and superconducting contacts. Another possibility is to use a nanowire deposited onto the ferromagnet and the superconductor [22]. This system is especially appealing since, e.g., InSb nanowires have large effective g factors. Then, for $\Delta_Z = g\mu_B B/2 = 2\Delta$ we estimate a magnetic field $B \simeq 5$ T using $g = 40$ and $\Delta = 3$ meV for Nb [39]. We then need a superconducting lead with high critical field B_c . Nb compounds precisely show the property that $B_c > B$. Then, we can neglect the dependence of Δ on the magnetic field to a first approximation. One could also envision a self-assembled quantum dot connected to two electrodes as in Ref. [40] or a break junction comprising a C_{60} molecule [41, 42]. The ferromagnetic electrode can be Joule heated with a slowly time-dependent electric current with zero average and thus leading to a temperature shift across the junction [11, 12]. Most of the applied temperature bias drops at ferromagnetic interface [8] and thus the superconducting temperature (and thereby its energy gap) is largely unaffected by the thermal gradient. The detection of the spin bias can be done using the inverse spin Hall effect [43]. Finally, the magneto-Seebeck effect needs the magnetization to be switched, which can be accomplished, e.g., by employing an external magnetic field that can be really small for soft ferromagnets.

Our work raises two important questions. First, what is the role of electron-electron interactions? Our theory assumes a single-level dot large enough that Coulomb repulsion is negligible. The results would also hold for strongly coupled quantum dots since in this case the charging energy U is smaller than the tunneling broadening and electronic interactions can be safely disregarded. However, small dots usually have large U and Coulomb blockade effects become dominant. It would be even possible to explore strongly correlated phenomena such as the Kondo effect [44, 45]. An Anderson-like Hamiltonian should be then used. The second question concerns the role of higher-order terms in the current-voltage or current-temperature characteristics [46, 47] and heat [48]. Even if larger temperature biases do not contribute to the Andreev current there appear cross terms that mix voltage and temperature differences [23]. In that case, one should resort to differential thermopowers and the results might change significantly. Our work is thus a first approach to a problem with fertile ramifi-

cations.

2014R1A6A3A03059105.

ACKNOWLEDGMENTS

This research was supported by MINECO under Grant No. FIS2014-52564 and the Korean NRF-

-
- [1] L. D. Hicks and M. S. Dresselhaus, Effect of quantum-well structures on the thermoelectric figure of merit, *Phys. Rev. B* **47**, 12727 (1993).
- [2] G. D. Mahan and J. O. Sofo, The best thermoelectric, *Proc. Natl. Acad. Sci. USA* **93**, 7436 (1996).
- [3] H. J. Goldsmid, *Introduction to Thermoelectricity* (Springer-Verlag, Berlin, 2010).
- [4] A. F. Ioffe, *Semiconductor Thermoelements and Thermoelectric Cooling* (Infosearch, London, 1957).
- [5] V. L. Ginzburg, Thermoelectric effects in the superconducting state, *Sov. Phys. Usp.* **34**, 101 (1991).
- [6] P. Machon, M. Eschrig, and W. Belzig, Nonlocal Thermoelectric Effects and Nonlocal Onsager relations in a Three-Terminal Proximity-Coupled Superconductor-Ferromagnet Device, *Phys. Rev. Lett.* **110**, 047002 (2013).
- [7] A. Ozaeta, P. Virtanen, F. S. Bergeret, and T. T. Heikkilä, Predicted Very Large Thermoelectric Effect in Ferromagnet-Superconductor Junctions in the Presence of a Spin-Splitting Magnetic Field, *Phys. Rev. Lett.* **112**, 057001 (2014).
- [8] S. Kolenda, M. J. Wolf, and D. Beckmann, Observation of thermoelectric currents in high-field superconductor-ferromagnet tunnel junctions, *Phys. Rev. Lett.* **116**, 097001 (2016).
- [9] M. S. Kalenkov and A. D. Zaikin, Electron-hole imbalance and large thermoelectric effect in superconducting hybrids with spin-active interfaces, *Phys. Rev. B* **90**, 134502 (2014).
- [10] P. Machon, M. Eschrig, and W. Belzig, Giant thermoelectric effects in a proximity-coupled superconductor-ferromagnet device, *New J. Phys.* **16**, 073002 (2014).
- [11] A. A. M. Staring, L. W. Molenkamp, B. W. Alphenaar, H. van Houten, O. J. A. Buyk, M. A. A. Mabeoone, C. W. J. Beenakker, and C. T. Foxon, Coulomb-Blockade Oscillations in the Thermopower of a Quantum Dot, *Europhys. Lett.* **22**, 57 (1993).
- [12] S. Fahlvik Svensson, E. A. Hoffmann, N. Nakpathomkun, P. M. Wu, H. Q. Xu, H. A. Nilsson, D. Sánchez, V. Kashcheyevs and H. Linke, Nonlinear thermovoltage and thermocurrent in quantum dots, *New J. Phys.* **15**, 105011 (2013).
- [13] T. E. Humphrey and H. Linke, Reversible Thermoelectric Nanomaterials, *Phys. Rev. Lett.* **94**, 096601 (2005).
- [14] M. Tinkham, *Introduction to Superconductivity* (McGraw-Hill, Singapore, 1996).
- [15] M. J. M de Jong and C. W. J. Beenakker, Andreev Reflection in Ferromagnet-Superconductor Junctions, *Phys. Rev. Lett.* **74**, 1657 (1995).
- [16] J. Aumentado and V. Chandrasekhar, Mesoscopic ferromagnet-superconductor junctions and the proximity effect, *Phys. Rev. B* **64**, 054505 (2001).
- [17] G. Deutscher and D. Feinberg, Coupling superconducting-ferromagnetic point contacts by Andreev reflections, *Appl. Phys. Lett.* **76**, 487 (2000).
- [18] G. Falci, D. Feinberg, and F. W. J. Hekking, Correlated tunneling into a superconductor in a multiprobe hybrid structure, *Europhys. Lett.* **54**, 255 (2001).
- [19] R. Mélin and D. Feinberg, Sign of the crossed conductances at a ferromagnet/superconductor/ferromagnet double interface, *Phys. Rev. B* **70**, 174509 (2004).
- [20] D. Beckmann, H. B. Weber, and H. v. Löhneysen, Evidence for Crossed Andreev Reflection in Superconductor-Ferromagnet Hybrid Structures, *Phys. Rev. Lett.* **93**, 197003 (2004).
- [21] D. Sánchez, R. López, P. Samuelsson, and M. Büttiker, Andreev drag effect in ferromagnetic-normal-superconducting systems, *Phys. Rev. B* **68**, 214501 (2003).
- [22] L. Hofstetter, A. Geresdi, M. Aagesen, J. Nygård, C. Schönenberger, and S. Csonka, Ferromagnetic Proximity Effect in a Ferromagnet-Quantum-Dot-Superconductor Device, *Phys. Rev. Lett.* **104**, 246804 (2010).
- [23] S.-Y. Hwang, R. López, and D. Sánchez, Cross thermoelectric coupling in normal-superconductor quantum dots, *Phys. Rev. B* **91**, 104518 (2015).
- [24] N. R. Claughton and C. J. Lambert, Thermoelectric properties of mesoscopic superconductors, *Phys. Rev. B* **53**, 6605 (1996).
- [25] Ph. Jacquod, R. S. Whitney, J. Meair, and M. Büttiker, Onsager relations in coupled electric, thermoelectric, and spin transport: The tenfold way, *Phys. Rev. B* **86**, 155118 (2012).
- [26] K. Uchida, S. Takahashi, K. Harii, J. Ieda, W. Koshibae, K. Ando, S. Maekawa, and E. Saitoh, Observation of the spin Seebeck effect, *Nature* **455**, 778 (2008).
- [27] A. Slachter, F. L. Bakker, J-P. Adam, and B. J. van Wees, Thermally driven spin injection from a ferromagnet into a non-magnetic metal, *Nat. Phys.* **6**, 879, (2010).
- [28] C. M. Jaworski, J. Yang, S. Mack, D. D. Awschalom, J. P. Heremans, and R. C. Myers, Observation of the spin-Seebeck effect in a ferromagnetic semiconductor, *Nature Materials* **9**, 898 (2010).
- [29] A. Cottet, T. Kontos, S. Sahoo, H. T. Man, M.-S. Choi, W. Belzig, C. Bruder, A. F. Morpurgo, and C. Schönenberger, Nanospintronics with carbon nanotubes, *Semicond. Sci. Technol.* **21**, S78 (2006).
- [30] X. Cao, Y. Shi, X. Song, S. Zhou, H. Chen, Spin-dependent Andreev reflection tunneling through a quantum dot with intradot spin-flip scattering, *Phys. Rev. B* **70**, 235341 (2004).
- [31] J. C. Cuevas, A. Martín-Rodero, and A. Levy Yeyati, Hamiltonian approach to the transport properties of superconducting quantum point contacts, *Phys. Rev. B* **54**, 7366 (1996).
- [32] Q.-F. Sun, J. Wang, and T.-H. Lin, Resonant Andreev reflection in a normal-metal-quantum-dot-superconductor system, *Phys. Rev. B* **59**, 3831 (1999).
- [33] M. R. Gäber, T. Nussbaumer, W. Belzig, and C. Schönenberger, Quantum dot coupled to a normal and a superconducting lead, *Nanotechnology* **15**, S479 (2004).
- [34] R. S. Deacon, Y. Tanaka, A. Oiwa, R. Sakano, K. Yoshida, K. Shibata, K. Hirakawa, and S. Tarucha, Tunneling Spectroscopy of Andreev Energy Levels in a Quantum Dot Coupled to a Superconductor, *Phys. Rev. Lett.* **104**, 076805 (2010);

- Kondo-enhanced Andreev transport in single self-assembled InAs quantum dots contacted with normal and superconducting leads, *Phys. Rev. B* **81**, 121308(R) (2010).
- [35] P. Trocha and I. Weymann, Spin-resolved Andreev transport through double-quantum-dot Cooper pair splitters, *Phys. Rev. B* **91**, 235424 (2015).
- [36] M. Misiorny and J. Barnaś, Effect of magnetic anisotropy on spin-dependent thermoelectric effects in nanoscopic systems, *Phys. Rev. B* **91**, 155426 (2015).
- [37] M. Misiorny and J. Barnaś, Spin-dependent thermoelectric effects in transport through a nanoscopic junction involving a spin impurity, *Phys. Rev. B* **89**, 235438 (2014).
- [38] M. Walter, J. Walowski, V. Zbarsky, M. Münzenberg, M. Schäfers, D. Ebke, G. Reiss, A. Thomas, P. Peretzki, M. Seibt, J. S. Moodera, M. Czerner, M. Bachmann, and C. Heiliger, Seebeck effect in magnetic tunnel junctions, *Nature Materials* **10**, 742 (2011).
- [39] M. T. Deng, C. L. Yu, G. Y. Huang, M. Larsson, P. Caroff, and H. Q. Xu, Anomalous Zero-Bias Conductance Peak in a Nb-InSb Nanowire-Nb Hybrid Device, *Nano Lett.* **12**, 6414 (2012).
- [40] G. Katsaros *et al.*, Hybrid superconductor-semiconductor devices made from self-assembled SiGe nanocrystals on silicon, *Nature Nanotech.* **5**, 458 (2010).
- [41] A. N. Pasupathy, R. C. Bialczak, J. Martinek, J. E. Grose, L. A. K. Donev, P. L. McEuen, and D. C. Ralph, The Kondo Effect in the Presence of Ferromagnetism, *Science* **306**, 86 (2004).
- [42] C. B. Winkelmann, N. Roch, W. Wernsdorfer, V. Bouchiat, and F. Balestro, Superconductivity in a single C₆₀ transistor, *Nature Phys.* **5**, 876 (2009).
- [43] E. Saitoh, M. Ueda, H. Miyajima, and G. Tatara, Conversion of spin current into charge current at room temperature: Inverse spin-Hall effect, *Appl. Phys. Lett.* **88**, 182509 (2006).
- [44] L. Li, Z. Cao, H.-G. Luo, F.-C. Zhang, and W.-Q. Chen, Fano resonance in a normal metal/ferromagnet-quantum dot-superconductor device, *Phys. Rev. B* **92**, 195155 (2015).
- [45] I. Weymann and K. P. Wójcik, Andreev transport in a correlated ferromagnet-quantum-dot-superconductor device, *Phys. Rev. B* **92**, 245307 (2015).
- [46] D. Sánchez and R. López, Scattering Theory of Nonlinear Thermoelectric Transport, *Phys. Rev. Lett.* **110**, 026804 (2013).
- [47] S.-Y. Hwang, D. Sánchez, M. Lee, and R. López, Magnetic-field asymmetry of nonlinear thermoelectric and heat transport, *New J. Phys.* **15**, 105012 (2013).
- [48] K. Yamamoto and N. Hatano, Thermodynamics of the mesoscopic thermoelectric heat engine beyond the linear-response regime, *Phys. Rev. E* **92**, 042165 (2015).